Laboratoire de Biorhéologie et d'Hydrodynamique Physique [1]), *U.E.R. de Physique – Université Paris VII*

Rheology of concentrated disperse systems
III. General features of the proposed non-newtonian model. Comparison with experimental data

D. Quemada

With 5 figures and 3 tables

1. Introduction

In a previous paper (1), a non-newtonian viscosity equation has been obtained using a semi-phenomenological approach. Volume concentration ϕ and shear rate $\dot{\gamma}$ dependences are found in the form

$$\eta_r = (1 - \tfrac{1}{2}\, \tilde{k}\, \phi)^{-2} \qquad [1.1]$$

where

$$\tilde{k} = \frac{k_0 + k_\infty \dot{\gamma}_r^p}{1 + \dot{\gamma}_r^p} \qquad [1.2]$$

is a generalized (shear dependent) intrinsic viscosity. If $k_0 > k_\infty$, shear-thinning is found, whereas shear-thickening corresponds to $k_0 < k_\infty$.

The functional form of [1.2] is derived from a phenomenologica kinetic model, except the exponent p of $\dot{\gamma}_r = \dot{\gamma}/\mathscr{D}_{\mathrm{Rot}} = kT\dot{\gamma}/8\,\pi\eta_F a^3$, that has to be empirically determined. Nevertheless, this p value is thought coming from the type of shear dependence of the effective diffusion coefficient D_{eff} of particles. Since non-spherical particles rotate in the shear rate $\dot{\gamma}$ with angular velocities which can be very different from $\dot{\gamma}/2$, mainly near the wall, it was argued in (1) that $D_{\mathrm{eff}} = \mathscr{D}_{\mathrm{Rot}}\, g(\dot{\gamma}_r)$, where $g(\dot{\gamma}_r)$ is an non-dimensional function of $\dot{\gamma}_r$. The same type of dependence in $\dot{\gamma}_r$ has been found yet for enhanced diffusion of small solute molecules by shear induced rotation of larger particles (2). A good agreement has been observed between this theoretical approach for platelet transport induced by Red Blood Cell (RBC) rotation (3) and experiments using labelled platelets (4).

Returning to [1.2], reasonable assumptions on D_{eff} lead to limit p to values such as $0 \le p \le 1$.

For various systems of rod- or disc-shaped particles, empirical values of p were found roughly between 0.4 and 0.6[2]). Taking for simplicity $p = 0.5$ in [1.2], gives the viscosity equation

$$\eta_r = \left(1 - \frac{1}{2}\, \frac{k_0 + k_\infty \dot{\gamma}_r^{1/2}}{1 + \dot{\gamma}_r^{1/2}}\, \phi\right)^{-2}. \qquad [1.3]$$

In the following sections, high shear and low shear rate limits will be discussed (Chap. 2 and 3, respectively). Pseudoplastic behaviour will be found with [1.3] when $\dot{\gamma}$ covers a large domain, including $\dot{\gamma}_c$. Checkings of experimental verification of [1.3] shows a fairly good agreement in several cases (Chap. 4), therefore backing up [1.3] as a relation having a rather large domain of applicability for systems of non-spherical particles (discs and rods, and in particular, RBC and rouleaux).

Nevertheless, for systems of spherical particles, the same approach leads to $g(\dot{\gamma}_r) = 1$, i.e. $p = 1$. Data for such a system is analysed and allows accurate particle size determinations (Chap. 5).

Rheological parameters for characterization of concentrated disperse systems: For shear-thinning behaviour (i.e. if $k_0 < k_\infty$), eq. [I.3.28][3]) – and more generally eq. [I.3.12] – contains explicit variations with both concentration ϕ

---

[1]) Equipe de Recherche Associé au C.N.R.S.

[2]) If data for an "individual" experiment are used. On the contrary a broader distribution of p ($0.2 \lesssim p \lesssim 0.8$) was found using data based on mean values (for η_F, ϕ, η), leading to a situation in some respect similar to polydispersity.

[3]) In the following eqs. [a.b] in paper (1) are referred to as [I.a.b].

and shear rate $\dot\gamma$, depending on three Rheological Parameters (RP), k_0, k_∞ and $\dot\gamma_c$. However, each of these depends on concentration (as it was met with already in newtonian case, Chap. 1 of (1)) and this leads to complicate data analysis of measurements of $\eta_r = \eta_r(\phi)$ vs. ϕ at constant shear rate. On the contrary, if ϕ is fixed, $\phi = \phi_1$, [I.3.28] — i.e. [1.3] — becomes a function of $\dot\gamma$ only, and a fit on experimental data must give the values of RP, which can be considered as a set of values *characterizing the structure* of the system at this fixed concentration ϕ_1. Several examples will be given in the following.

2. High shear rate limit, $\dot\gamma \gg \dot\gamma_c$ (5) comparison with Casson's law

Using the shear stress $\sigma = \eta\dot\gamma$, [1.3] can be rewritten as

$$\sigma^{1/2} = \frac{\eta_F\dot\gamma^{1/2}}{1 - \frac{1}{2}\tilde k\phi} \qquad [2.1]$$

where

$$\tilde k = \frac{k_0 + k_\infty(\dot\gamma/\dot\gamma_c)^{1/2}}{1 + (\dot\gamma/\dot\gamma_c)^{1/2}}. \qquad [2.1a]$$

If $\dot\gamma \gg \dot\gamma_c$, expansion into a serie in $(\dot\gamma/\dot\gamma_c)^{1/2}$ gives

$$\sigma^{1/2} = \frac{\eta_F^{1/2}}{1 - \frac{1}{2}k_\infty\phi}\dot\gamma^{1/2}$$
$$+ (\eta_F\dot\gamma_c)^{1/2}\frac{\phi}{2}\frac{k_0 - k_\infty}{(1 - \frac{1}{2}k_\infty\phi)^2}$$
$$+ \mathcal{O}\left[(\dot\gamma/\dot\gamma_c)^{-1/2}\right]. \qquad [2.2]$$

As would be expected, since [2.2] holds for suspensions of rod-like particles, this reproduces Casson's relation [I.3.23], i.e.

$$\sigma^{1/2} = K^{1/2}\dot\gamma^{1/2} + \sigma_0^{1/2} \qquad [2.3]$$

with a *Casson viscosity* K and a *yield shear stress* σ_0 such as

$$K = \eta_F(1 - \tfrac{1}{2}k_\infty\phi)^{-2} = \eta(\dot\gamma \to \infty) \equiv \eta_\infty, [2.4]$$

$$\sigma_0 = \frac{1}{4}\eta_F\dot\gamma_c(k_0 - k_\infty)^2\frac{\phi^2}{(1 - \tfrac{1}{2}k_\infty\phi)^4}. \qquad [2.5]$$

These expressions are comparable with those calculated by *Casson* (6) using an orientation parameter a (related to initial distribution of rod orientation, when flow begins) and two shape parameters β_1 and β, yet introduced at

the end of Chap. 3.5 (1). Putting for convenience $q = a\beta_1 - 1$, Casson theory gives

$$K^{\text{Casson}} = \eta_F(1 - \phi)^{-q}, \qquad [2.6]$$

$$\sigma_0^{\text{Casson}} = \left(\frac{a\beta}{q}\right)^2\left[(1 - \phi)^{-q/2} - 1\right]^2 \qquad [2.7]$$

where the concentration dependence, as $(1 - \phi)$ — which implies a packing concentration equal to 1 — was found by *Casson* when he used the *Brinkman-Roscoe* method to extend his theory for moderately dilute suspensions to highly concentrated ones. Discarding the latter, [2.6] and [2.7] become, after linearization in ϕ

$$K^{\text{Casson}} = \eta_F(1 + q\phi), \qquad [2.6a]$$

$$\sigma_0^{\text{Casson}} = \tfrac{1}{4}(a\beta)^2\phi^2, \qquad [2.7a]$$

which are very similar to the corresponding eqs. [2.4] and [2.5], in the same (dilute) limit, particularly with respect to a yield stress proportional to ϕ^2:

$$K = \eta_F(1 + k_\infty\phi), \qquad [2.4a]$$

$$\sigma_0 = \tfrac{1}{4}\eta_F\dot\gamma_c(k_0 - k_\infty)^2\phi^2. \qquad [2.5a]$$

Eqs. [2.6] and [2.7] apply to concentrated suspensions or deformable particles, like RBC suspensions of Blood whose packing concentration is close to $\phi_M = 1$. These systems have been shown to verify with high accuracy the Casson equation up to $\dot\gamma \sim 100\,\text{sec}^{-1}$ for a large range of concentrations, see *Brooks* et al. (7). Earlier, studying the action of fibrinogen, that initiated the RBC rouleaux formation. *Merrill* et al. (8) performed such a verification of [2.3], and determined the parameters β_1 and β in [2.6] and [2.7] from Couette viscometry data. The analysis of several samples of normal blood [table 1 in (8)] gives values of $q/2$ close to unity, with an average value $\bar q = 1.97$, which agrees with the exponent 2 in [2.4], in spite of large variations in fibrinogen concentration C_F. Variations of $\sigma_0^{1/2}$ vs. ϕ for different values of C_F observed by *Merrill* et al. (8) are shown on figure 1, and are compared to (2.5) with RP values for normal blood deduced from other data ($\phi = 0.419$, $k_0 = 4.68$, $k_\infty = 1.80$, $\dot\gamma_c = 2.0$). The agreement is rather satisfying. Nevertheless, the existence of so high yield stresses is questionable in RBC systems, and many studies have found negligeable values of σ_0 as $\dot\gamma \to 0$.
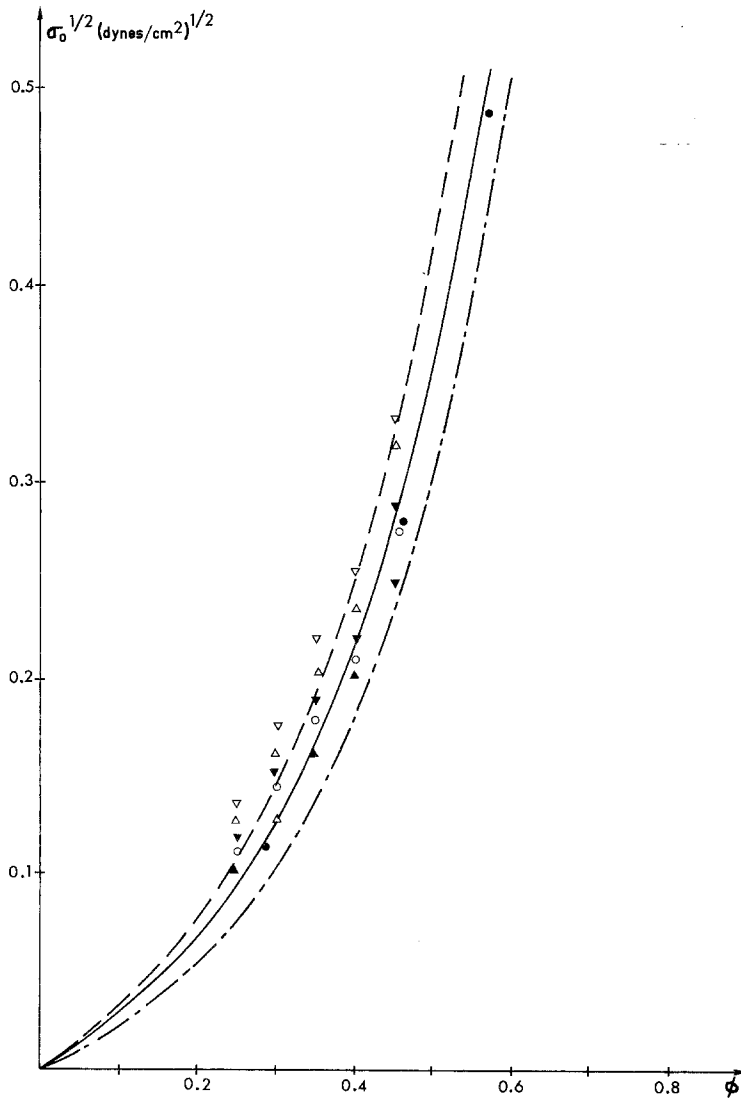
Fig. 1. Pseudo-yield stress σ_0.
Data of *Merrill* et al. (8)

Sample	Fibrinogen concentration [g/100 ml]	
K 6802	0.21	▲
K 4782	0.24	○, ●
K 2380	0.27	▼
K 5834	0.35	△
K 4370	0.46	▽

Curves (eq. [2.5])

	η_r (cP)	k_0	k_∞	$\dot{\gamma}_c$ sec^{-1}
– – – –	2.0	3.06	1.80	9.18
–·–·–	1.7	3.24	1.80	4.00
———	1.2	4.68	1.80	2.04

3. Low shear limit $\dot{\gamma} \ll \dot{\gamma}_c$

If $\dot{\gamma}_r \ll 1$, eq. [1.3] becomes

$$\eta_r^{1/2} = \eta_{r_0}^{1/2}\left[1 - (k_0 - k_\infty)\eta_{r_0}^{1/2}\frac{\phi}{2}\dot{\gamma}_r^{1/2}\right]$$
$$+ \mathcal{O}(\dot{\gamma}_r) \qquad [3.1]$$

where η_{r_0} is the zero-shear relative viscosity

$$\eta_{r_0} = (1 - \tfrac{1}{2}k_0\,\phi)^{-2}. \qquad [3.2]$$

From [3.1]

$$\sigma = \eta_F\eta_{r_0}\dot{\gamma} + \mathcal{O}(\dot{\gamma}_r^{3/2})$$

which does not exhibit any yield stress at $\dot{\gamma} = 0$. On the contrary, as $\dot{\gamma} \to 0$, newtonian behaviour is recovered. Nevertheless, in highly concentrated media, one can presume that particles

and/or aggregates can form a three-dimensional network at rest, i.e. a gel-like structure, having some yield stress. In [3.1], the absence of the latter at $\dot{\gamma} = 0$ comes from that such effects are not taken into account in the present model. However, such a model will be correct if the yields stress has an extremely small magnitude, due to the smallness of cohesive forces between particles. This is what happens with normal blood, where the network, formed at rest by rouleaux, is very easy to disrupt in individual rouleaux.

Relaxation time: Furthermore, squaring [3.1] yields

$$\eta_r = \eta_{r_0}\left[1 - (k_0 - k_\infty)\eta_{r_0}^{1/2}\phi\dot{\gamma}_r^{1/2}\right]$$
$$+ \mathcal{O}(\dot{\gamma}_r). \qquad [3.3]$$

This variation in function of $\dot{\gamma}_r^{1/2}$ can be supported by a more rigorous theory in this low shear limit. *Bueche* (9) calculated the viscosity of high polymers in dilute and concentrated solutions. He has considered the polymer coil as an array of elastically coupled segments, each of them subject to shear stresses and thermal agitation depending on its surrounding. For a free draining coil, at very high dilution, variation with $\dot{\gamma}_r^2$ is recovered. With high molecular weights, taken into account solvent immobilization within the coil, *Bueche* introduced a shielding factor which reduces the shear rate inside of the coil. In dilute solutions, at very low $\dot{\gamma}$, the resulting viscosity η is obtained (9) as

$$\eta - \eta_r = (\eta_0 - \eta_F)\left[1 - (\tau_B \dot{\gamma})^{1/2}\right] + \mathcal{O}(\dot{\gamma}) \quad [3.4]$$

where $\eta_0 = \eta(\dot{\gamma} = 0)$, and τ_B is a relaxation time, given by

$$\tau_B = 3.72\,(\eta - \eta_F)\,\frac{(m\,m_0)^{1/2}}{kTc}\,. \quad [3.5]$$

c being the weight concentration of solute, and m_0, m, the masses of a segment and of a molecule, respectively. *Bueche* pointed out that [3.4] "fits the available experimental data surprisingly well". This good agreement is obtained "without the use of arbitrary parameters, although the data were taken on different polymers, at various temperatures, in various solvents, by independent investigators". For concentrated solutions and bulk polymers, *Bueche* approximated his free draining solution taking the suspending fluid viscosity negligeable in comparison with η_F. If we apply this approximation to his "shielding" results [3.4], assuming that it holds for concentrated solutions, we obtain

$$\eta = \eta_0\left[1 - (\tau_B \dot{\gamma})^{1/2}\right] \quad [3.4\mathrm{a}]$$

where

$$\tau_B = 3.72\,\eta\,\frac{(m\,m_0)^{1/2}}{kTc}\,. \quad [3.5\mathrm{a}]$$

Eq. [3.3] has the same form as [3.4a], with a relaxation time

$$\tau_R = (k_0 - k_\infty)^2 \eta_{r_0}\,\phi^2/\dot{\gamma}_c \quad [3.6]$$

which can be compared to [3.5a]. This leads to define a critical shear rate $\dot{\gamma}_c$, as in [I.3.16], by

$$\dot{\gamma}_c = \frac{kT}{\beta_p \eta_F R^3} \quad [3.7]$$

where β_p depends on $k_0 - k_\infty$, on N, the number of segments in a molecule (having an effective radius R) and on α_e, the molecular expansion factor.

Pseudo-yield stress: At high concentration, and more especially if ϕ is near the packing value $\phi_M = 2/k_0$, the viscosity η_{r_0}, defined by eq. [3.2], is very large. As η_{r_0} is the slope of the curve at $\dot{\gamma} \to 0$, the variation of σ against $\dot{\gamma}$, which results from [2.1], is very close to that the Casson equation gives. Then σ_0 appears as a *pseudo-yield stress*. (Note that the same approximation would be obtained with a Bingham material.)

4. Pseudo-plastic behaviour. Method of characterization

If a given media is studied using a given viscometer, its rheological behaviour will depend on the value of $\dot{\gamma}_c$ compared to the range of shear rate values the viscometer allows, from $\dot{\gamma}_1$ to $\dot{\gamma}_2$. If $\dot{\gamma}_c < \dot{\gamma}_1$, the high shear limit [2.2] will be observed, i.e. the Casson equation will be verified, with a newtonian behaviour at very high shear rates. Since $\dot{\gamma}_c \sim a^{-3}$ such a behaviour is met with in suspensions of particles large in size, as ordinary suspensions ($a \gg 1\ \mu\mathrm{m}$). On the contrary, for $\dot{\gamma}_c > \dot{\gamma}_2$, one will see the low shear limit behaviour [3.1], as is exhibited by solutions of ordinary solutes or very low molecular weight polymer ($a \ll 10^{-2}\ \mu\mathrm{m}$). Complete pseudo-plastic behaviour requires $\dot{\gamma}_1 < \dot{\gamma}_c < \dot{\gamma}_2$ to be observed, i.e. systems like suspensions of colloidal particles, like very high molecular weight polymers in poor solvents, or like microemulsions, with $10^{-2} \lesssim a \lesssim 1\ \mu\mathrm{m}$. Non-rigid-particles suspensions, high polymers in good solvents or emulsions, can show more complex behaviour, although analogous.

Fitting the general eq. [1.3] on experimental data enable the RP values, k_0, k_∞ and $\dot{\gamma}_c$, to be determined. It can be expected that k_0, which dominate the zero-shear rate behaviour, mainly depicts aggregation properties of the system, while k_∞ describes the high shear rate (newtonian) limit, and, through deviations from Einstein value for spheres, depends on size, thus on orientation and deformation of particles and hence, on suspending fluid viscosity. Finally, $\dot{\gamma}_c$ is sensitive to effective volume of particles and, whether particles are deformable, to their mechanical properties (elasticity, "internal" viscosity, etc.). Some examples will be given now.
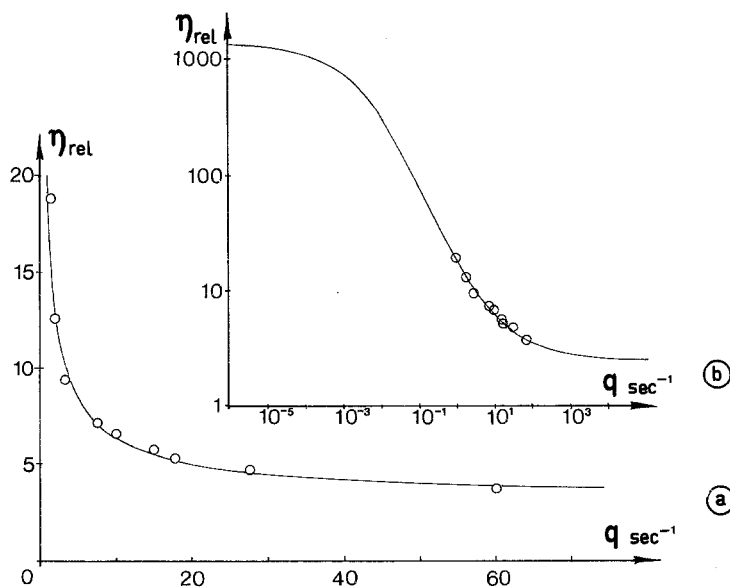
Fig. 2. Non-newtonian behaviour of flexible particle suspension: ○ *Sacks'* and *Tickner'*s data (10), ———— theoretical variations according [1.3] with $k_0 = 5.134$, $k_\infty = 2.117$, $\dot{\gamma}_c = 1.84 \sec^{-1}$.
a) High shear rate variations, showing shear thinning behaviour;
b) including very low shear rate, showing "generalized newtonian fluid" properties

4.1. Suspensions of flexible particles in highly viscous fluid

Figure 2 shows variations of $\eta_r(\dot{\gamma}_r)$, measured by *Tickner* and *Sacks* (10) on a concentrated suspension ($\phi = 0.40$) of flexible discs (diameter = 5.55 mm, thickness = 1.3 mm) made with polyacrylamide gel, suspended in a high viscosity newtonian fluid ($\eta_F = 4.88$ P.). If [1.3] is fitted to the corresponding data, RP-values are found to be

$$k_0 = 5.134, \qquad k_\infty = 2.117,$$

$$\dot{\gamma}_c = 1.84 \sec^{-1}. \qquad\qquad [4.1]$$

The $\dot{\gamma}$-range studied is too restricted to give precise values of RP at very low shear rate, but value of k_∞, smaller than the Einstein one, must be related to orientation effects. Moreover, $\dot{\gamma}_c \sim 2 \sec^{-1}$ cannot be related to [I.3.16] since such large particles have a very low "rotational $\dot{\gamma}_c^R$", (from [I.3.16], with $\beta = 8\pi$. $\dot{\gamma}_c^R \simeq 2 \cdot 10^{-5}$ $\sec^{-1}$). On the other hand, taking $2 \sec^{-1}$ as the value of the "elastic critical shear rate", given in [I.3.18] and using the measured elastic modulus, $E = 5 \cdot 10^{-4}$ dynes/cm^2, yields a very high viscosity ($\eta_i \simeq 3 \cdot 10^4$ Poises), which is a plausible value for such an acrylamide gel. — The value of η_i is not given in ref. (10).

4.2. Blood and RBC suspensions

Blood and RBC suspensions exhibit very strong non-newtonian effects if $\dot{\gamma}$ becomes smal-

ler than about $10 \sec^{-1}$. As has been yet stressed on, these effects are dominated at low $\dot{\gamma}$ by aggregation-disaggregation equilibrium, while at high $\dot{\gamma}$ they are governed by orientation-disorientation equilibrium, and eventually (with non rigid particles) by deformation-undeformation equilibrium.

Checked modification of these factors, aggregability and deformability, can be reached considering abnormal (either pathological or artificial) situations. This promotes development of rheological studies on blood and RBC suspensions[4]. Some illustrative results will be shown in the following.

---

[4] Although Blood and RBC suspensions appear as very complex systems they present *under normal conditions* many advantages for the study of non-newtonian behaviour. Indeed, the particles they contain have precise properties (in the sense of small deviations from mean values) and are suspended in a fluid (the plasma) having well defined physicochemical state. The most important features are the following: (i) The size of RBC corresponds to a very narrow calibration. (ii) Their extreme deformability (however associated to a large resistance to area changes), allows strong orientation effects by flow, discarding too high $\dot{\gamma}$ values for avoid of any inertial effect or hemolysis. (iii) Aggregates of RBC possess a characteristic shape, the so-called "rouleau-shape", and the aggregation mechanism does not seem to depend on the number of RBC in the rouleau, but mainly an RBC-RBC interaction, the latter varying with physicochemical properties of suspending fluid. (iv) Relaxation times associated with Brownian rotation are very large and the observed time is the one associated with deformation (and the resulting orientation) of the order of $0.1 - 1$ sec.

1) Figure 3 shows variations of $\sigma^{1/2} = f(\dot{\gamma}^{1/2})$ according to eq. [2.2] fitted on data of *Merrill* et al. (8), for whole Blood and RBC in defibrinated plasma: pseudo-yield stress is clearly shown for the former, but does not exist for the latter.
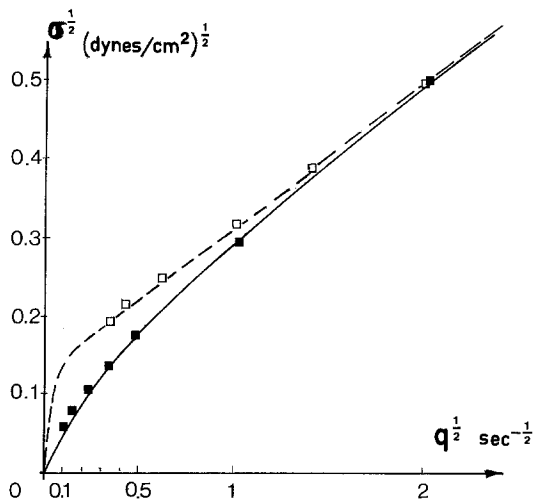

Fig. 3. Non newtonian behaviour of blood ($\square$) and red cells in defibrinated plasma ($\blacksquare$): Data from *Merrill* et al. (8); theoretical variations, according [1.3] with

Table 1.

	η_r [P]	k_∞	k_0	$\dot{\gamma}_c$ sec^{-1}	ϕ	
Blood	0.012	1.8	4.68	0.69	0.419	$- - -$
RC in Fract. IV	0.014	1.8	3.96	1.23	0.406	$\underline{\quad\quad}$

2) Measurements by *S. Chien* (11) on three suspensions [(i) NP = Normal RBC in plasma, (ii) NA = Normal RBC in 11% albumin-Ringer, (iii) HA = Hardened RBC in 11% albumin Ringer] having the same volume concentration ($\phi = 0.45$) and the same suspending fluid viscosity ($\eta_F = 1.2$ cP), have been performed to separate the effects that RBC aggregation and RBC deformation exert on viscosity and especially on its variations with respect to shear rate. Fitting [1.3] to this data leads to RP-values shown in table 1.

Table 1. Rheological parameters for non-newtonian behaviour of RBC suspensions $\phi = 0.45$, $\eta_F = 1.2$ cP

	k_∞	k_0	$\dot{\gamma}_c$ sec^{-1}	ϕ_M
NP	1.78	4.20	5.0	0.476
NA	1.78	3.29	25.0	0.608
HA	3.62	—	—	0.552

Such values call for the following comments:

(i) $k_\infty = 1.78$ both for NP and NA: This agrees with the same deformation of normal RBC (expected, since both concentration ϕ and average viscosity η_F are the same). Furthermore, this value is very close to that other samples of normal blood gave (5, 12). Note that in this very high shear limit $\dot{\gamma} \gg \dot{\gamma}_c$, at high concentration, one can expect a particle alignment with flow, very close to its maximum level.

(ii) Aggregation effects appear in $k_0^{NP} = 4.20$, for NP, in comparison with $k_0^{NA} = 3.29$, for NA, since the latter, in which plasma proteins (fibrinogens and globulins) responsible of RBC aggregation are absent, does not present such effects. Moreover, for NA, packing concentration $\phi_M = 2/k_0^{NA}$ (defined as in [1.1.4] but, evidently, using rest value k_0^{NA}) is $\phi_M^{NA} = 0.607$, close to the value $\Phi_M = 0.61 \pm 0.01$ drawn from centrifugation measurements using labelled plasma (13) and agrees with $\varphi_M = 0.59$ obtained for close packing of discoids (14) modeling undeformed RBC [5].

(iii) In NP, $\dot{\gamma}_c = 5.0$ sec^{-1} agrees surprisingly well with the value given in [I.3.19] from the data of *Skalak* for shear elasticity and viscosity of RBC membrane. As RBC aggregation mechanism seems to have to be explained by bridging of partially absorbed macromolecules onto RBC surfaces, as *Chien* et al. (15) pointed out, one can conclude that RBC membrane properties dominate the effective mechanical properties of a rouleau. Nevertheless, using $E_i \sim a^{-3}$ as in polymer chains, see Chap. 3.4.b in (1), one could expect a lowered shear elasticity but associated with a lowered "internal viscosity", the latter mainly resulting from polymer bridges. Moreover, the enhanced value $\dot{\gamma}_c = 25$ sec^{-1} found in NA suggests to associate modifications of effective "membrane" properties with changes in both ion and protein content of plasma, such changes inducing well-known modifications of the RBC aggregation level. On one hand, it will be possible that, in Ringer, ionic adsorption onto RBC surfaces leads to an increase in E_i, hence in $\dot{\gamma}_{ci}$. On the other hand, taking again $E_i \sim a^{-3}$ the ratio $\dot{\gamma}_c^{NA}/\dot{\gamma}_c^{NP} = 5$ could be related (21) to an approximate number n of RBC per

[5] Then, higher packing for deformable RBC could be associated to some deformation effect by crowding: at $\phi = 0.45$, this gives a reduction of $(\Phi_M - \varphi_M)(1 - \varphi_M) = 5\%$ of the void volume between particles.

Table 2. Comparison of observed and (from [1.3]) calculated viscosities

	ϕ	η_F cP	k_∞	k_0	$\dot{\gamma}_c$ sec^{-1}	apparent viscosity (cP) obs. (20)	calc.	obs. (20)	calc.
Normal blood (17)	0.40 0.45	1.2 1.2	1.84 2.07	4.65 4.33	2.23 1.88	at $\dot{\gamma} = 0.1\ \text{sec}^{-1}$ 42.6 ± 11.6 35.3 67.3 ± 12.3 68.2		at $\dot{\gamma} = 230\ \text{sec}^{-1}$ 3.6 ± 0.3 3.0 4.1 ± 0.5 4.1	
Sickle cell anemia (18)	40	1.4	2.83	4.63	4.94	at $\dot{\gamma} = 0.1\ \text{sec}^{-1}$ 68 ± 19 70.8		at $\dot{\gamma} = 230\ \text{sec}^{-1}$ 5.1 ± 0.6 6.64	
Packed cells (19)	0.88	1.2	1.83	2.26	2.16	apparent fluidity (Poise^{-1}) at $\dot{\gamma} = 2.30\ \text{sec}^{-1}$ 0.61 0.86		$\dot{\gamma} = 230\ \text{sec}^{-1}$ 1.51 2.64 (observed at $\phi = 0.95$)*)	

*) In the third case, RP-values are not known at $\phi = 0.95$, used in observations. Then, calculated values of fluidity, for $\phi = 0.88$, are somewhat higher than the observed ones.

rouleau about $n = 15$, in accordance with observations ($n \simeq 10 - 15$).

(iv) Finally, $k_\infty^{\text{HA}} = 3.62$ for HA agrees with findings in flowing suspensions of rigid particles, i.e. it corresponds to packing concentration allowing slip of adjacent layers of particles. − Recall, for instance, $\phi_M = 0.525$, $k = 3.81$, for cubic packing of hard spheres (25). − Here, a discoid packing ($\phi_M = 0.55$) is obtained, as evidence, denser than the sphere packing. Furthermore, dilatancy is observed at low shear rates for HA. − Note in measurements by *Chien* (11) the fall in relative viscosity as $\dot{\gamma}$ decreases below 0.1 sec^{-1}. Similar finding has been observed more recently by *Schmid-Schönbein* (16): for hardened RBC, RP-parameters take the following values $k_0 = 3.23$, $k_\infty = 3.97$. Again, dilatancy is clearly observed with high shear packing value $\phi_{M\infty} = 0.504$ weaker than the low shear one $\phi_{M0} = 0.619$. Moreover, the latter is close to that obtained for NA, $\phi_{M0}^{\text{NA}} = 0.61$, i.e., for undeformed and very weakly-aggregated particles, then indistinguishable from hardened cells.

Other RP-determinations, using various data, have led to very coherent findings (12). To illustrate this, table 2 gives, on one hand, RP-determinations for different systems:

(i) Normal blood, at $\phi = 0.40$ and 0.45 (from data of *Schmid-Schönbein* et al. (17)).

(ii) Sickle cells, i.e. RBC having abnormal Hemoglobin, hardened when desoxygenated, but which recovers some flexibility when oxygenated (from data of *Schmid-Schönbein* and *Wells* (18)).

(iii) Packed cells, at $\phi = 0.88$ (from data of *Usami* et al. (19)).

On the other hand, comparison between η (or $1/\eta$) calculated from these RP-values, and those directly observed by *Schmid-Schönbein* et al. (20) is shown.

As expected, RP-values appear as concentration dependent. Nevertheless, working at fixed volume concentration, their determination has been proposed as an attempt to system characterization (21, 23).

Finally, figure 4 displays another preliminary finding, using [1.3], related to electroviscous effects, which emphasizes aggregation effects. *Brooks* et al. (22) performed viscosity measurements on saline suspensions of human RBC to which high molecular weight Dextran has been added, at variable concentration C_{Dx}. These authors studied the conditions under which RBC were aggregated, with the help of a viscosity ratio R defined by

$$R = \frac{\eta(C_{Dx}, C_m)}{\eta} \cdot \frac{\eta(\text{Saline})}{\eta_F}.$$

Such a ratio compares viscosity measured [6]) at a fixed shear rate $\dot{\gamma}$ and hematocrit H, in presence of Dextran and at variable ionic strength C_m, to corresponding viscosity at the same $\dot{\gamma}$ and H, but in saline. For $H = 50$ and $\dot{\gamma} = 0.17\ \text{sec}^{-1}$, *Brooks* et al. gave variations of R vs. C_{Dx} and C_m, shown in figure 4a. At fixed $C_{Dx} = 3\ \text{gr}/100\ \text{ml}$, RP-values have been determined at ionic molar concentrations C_m used in (22). Corresponding k_0 values are given in table 3.

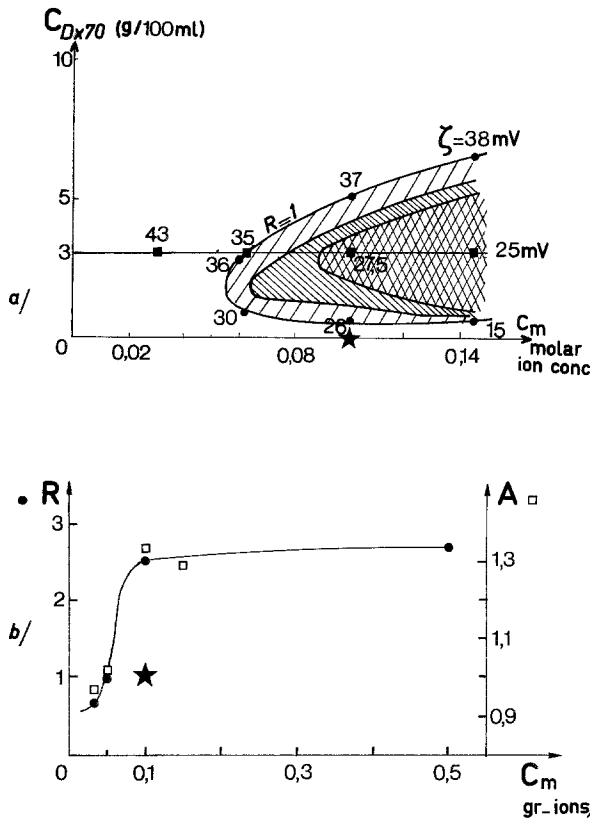[6]) More precisely, values of η obtained after fitting [I.3.21a] on viscosity data.

C_{Dx70} (g/100ml)

Fig. 4. Electroviscous effects and aggregation of Red Blood Cells.
a) Curves R = Const. (in Dx T 70 concentration and ionic strength C_m coordinates) and associated ζ-potential (from *Brook*'s data, fig. 5 in (22), using light microscopy observations). ● Limit $R = 1$. From viscosity data (22): ■ experiments at $C_{Dx70} = 3$ g/100 ml. (✦ Control in saline)
b) Variations of RBC "aggregation index A", calculated by fitting [1.3] on viscosity data (22), compared with corresponding R variations (from fig. 6 in (22)). □ = A values, ● = R values

Table 3. RBC aggregation index A

C_{Dx}	0.03				0.00
C_m	0.030	0.060	0.100	0.145	0.100
k_0	2.85	3.01	3.94	3.78	$2.94 = k_0^0$
$A = k_0/k_0^0$	0.97	1.02	1.34	1.29	1.00

Taking $k_0^0 = 2.94$ (for $C_{Dx} = 0$) as reference, one can roughly define a RBC aggregation index by $A = k_0/k_0^0$, values of which are given in table 3. Variations of A, shown on figure 4b, appear close to R-variations. The main advan-

tage of using A instead of R stays in that the former is by definition independent on shear while the latter is strongly shear dependent; see figure 3 in (22). The points which correspond to these values of C_{Dx} and C_m are located on figure 4a, inside different area for which light microscopy has shown different levels of RBC aggregation: these locations are in good agreement with corresponding A-values. Nevertheless, further analysis will be necessary for more precise interpretations of such an "aggregation index".

5. Dispersions of uniform colloidal spheres in non-aqueous media: An example of a system of class $p = 1$

Papir and *Krieger* (24) have measured non-newtonian viscosities of monodisperse spheres of polystyrene latexes (0.15 ≤ a ≤ 0.43 μm) suspended in benzylalcohol or in *m*-cresol. For constant concentration, they used eq. [I.3.22] to fit their experimental data by the method of least squares. After reduction of various data to a single one by using the reduced shear stress $\sigma_r = \sigma a^3/kT$, *Papir* and *Krieger* obtained limiting viscosities η_{r1} and η_{r2} as functions of volume concentration ϕ, satisfying the newtonian relations [I.3.2] or [I.3.3].

A test of [1.3] has been performed using data for a suspension of spheres having a diameter $2a = 0.155$ μm, immersed in benzyl-alcohol ($\eta_F = 4.89$ cP) at $\phi = 0.50$. The RP-determination gives (see figure 5)

$$k_0 = 3.288, \qquad k_\infty = 2.707,$$

$$\dot{\gamma}_c = 61.65 \text{ sec}^{-1}. \qquad [5.1]$$

The corresponding values for the limiting viscosities are

$$\eta_{r_0} = 31.56, \qquad \eta_{r_\infty} = 9.57 \qquad [5.2]$$

which are not in good agreement neither with measured values ($\eta_{r_0} = 24.0$; $\eta_{r_\infty} = 11.0$) nor predicted ones ($\eta_{r_0} = 24.7$; $\eta_{r_\infty} = 11.17$), see table 1 in (24). Moreover, the calculated curve, using [5.1], clearly appears (fig. 5) as a rather bad fitting. Indeed, such a discrepancy is not very surprising since dispersions considered here contain spherical particles, that could lead to $p \neq \frac{1}{2}$. As in Chap. 3.6 of (1), the best linear fit of [1.1] − [1.2] on the data of (24) gives the
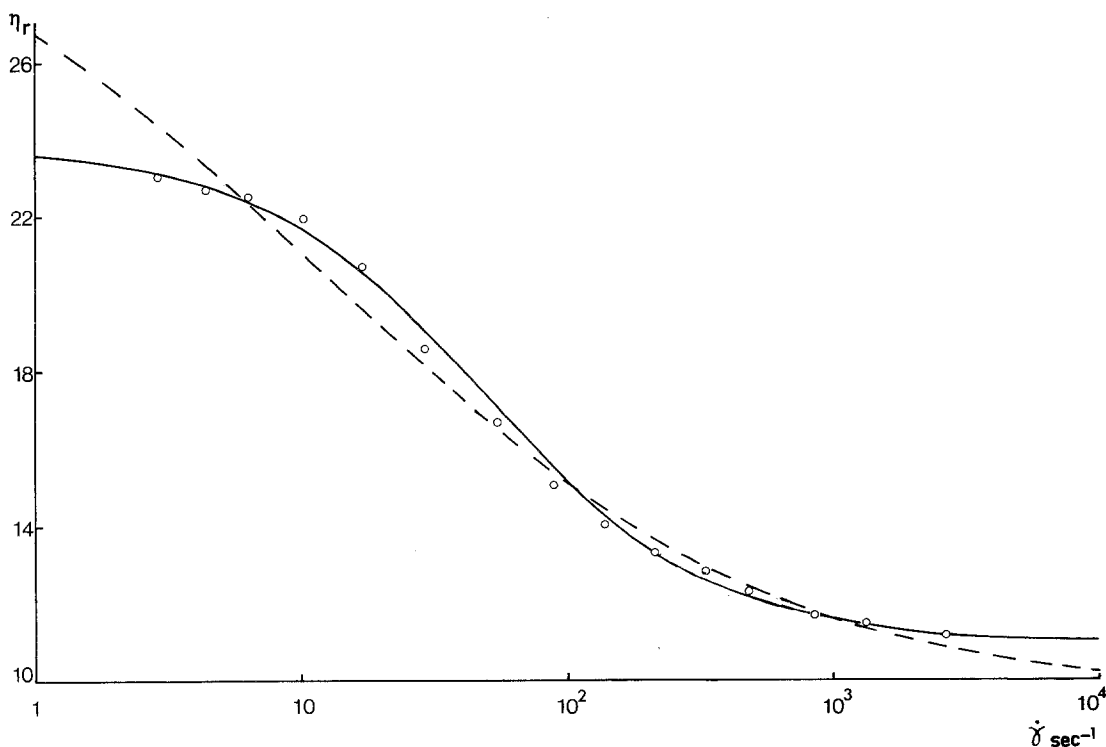
Fig. 5. Pseudo-plastic behaviour of monodisperse suspensions (polystyrene spheres in non-aqueous media) data from (24) ($\phi = 0.50$; $\eta_F = 4.89$ cP), curves (best fitted ———), using [1.1]−[1.2] with $\theta = (\dot{\gamma}/\dot{\gamma}_c)^p$:

	p	$k_0 = \kappa\alpha_0$	$k_\infty = \kappa\alpha_\infty$	$\dot{\gamma}_c$ sec^{-1}	
– – – – –	0.5	3.288	2.707	69.65	(i.e. with [1.3])
———————	~1	3.180	2.797	88.10	

best p value and corresponding RP-values. The results are

$$p = 0.986, \quad k_0 = 3.180, \quad k_\infty = 2.793,$$

$$\dot{\gamma}_c = 88.49 \text{ sec}^{-1} \qquad [5.3]$$

which call for the following remarks:

(i) As has been stressed in Chap. 3.6 of (1), several effects influence the p-value, among them can be found, as we have yet suggested, the deviation between vorticity of the suspending fluid and angular velocity of particles, when they are non-spherical ones. Nevertheless, such a deviation cannot exist for rigid spheres, leading to $p = 1$, according to [5.3].

(ii) Using k_0- and k_∞-values [5.3], one can calculate the corresponding values η_{r_0} and η_{r_∞} as

$$\eta_{r_0} = 23.79, \quad \eta_{r_\infty} = 10.98 \qquad [5.4]$$

in better agreement with the measured values than [5.2].

(iii) Since we are analysing properties of monodisperse suspensions of rigid spheres, one can estimate from [I.3.16] effective particle diameter $2a_{eff}$ taking $\dot{\gamma}_c = \mathcal{D}_{Rot} = kT/8\pi\eta_F a_{eff}^3$ or $\dot{\gamma}_c = \mathcal{D}_{Tr}/a_{eff}^2 = kT/6\pi\eta_F a_{eff}^3$. One finds

$$2a_{eff}^{Rot} = 0.1449 \text{ μm}, \quad 2a_{eff}^{Tr} = 0.1595 \text{ μm} \quad [5.5]$$

in fairly good agreement to the true value $2a = 0.155$ μm.

Similar analysis for other suspensions leads to results in accordance with [5.3]−[5.5]. For example, with same particles of diameter $2a = 0.155$ μm but suspended in m-cresol ($\eta_F = 17.38$ cP), one obtains

$$p = 1.048, \quad k_0 = 3.159, \quad k_\infty = 2.821,$$

$$\dot{\gamma}_c = 24.62 \text{ sec}^{-1}$$

hence

$$2a_{eff}^{Rot} = 0.1455 \text{ μm} \quad \text{and} \quad 2a_{eff}^{Tr} = 0.1601 \text{ μm}$$

in very good agreement with [5.5]. For particles having another diameter ($2a = 0.220\,\mu m$) in benzyl-alcohol, one finds

$$p = 1.177, \quad k_0 = 3.124, \quad k_\infty = 2.802,$$

$$\dot{\gamma}_c = 37.61\,\sec^{-1}$$

leading again to good agreement between effective diameters

$$2a_{\text{eff}}^{\text{Rot}} = 0.193\,\mu m\,; \quad 2a_{\text{eff}}^{\text{Tr}} = 0.212\,\mu m$$

and the true ones.

Such results allow to expect that, in monodisperse systems of well-defined spherical particles, but with unknown radius, as micro-emulsions, it might be possible to obtain size estimations from "critical-shear rate" determinations based on data processing of steady viscosity measurements.

6. Conclusion

The present study seems to produce two general results:

(i) Compared with the use of values of viscosity, even at very low shear rate, the proposed method, based on RP-determination, could present some advantages, the most important, after taking into account concentration dependence, being to separate aggregation and orientation-deformation of particles. Indeed, such a separation, although very crude — since using only three parameters — is possible because at $\dot{\gamma}_r \ll 1$, particle deformation disappears, as particle aggregation does at "infinite" shear rate, $\dot{\gamma}_r \gg 1$, and thus, calculated values of k_0 and k_∞ roughly reveal these effects, respectively. In contrast to this, for any finite value of $\dot{\gamma}$, measured values of viscosity take into account both these effects, mixed in variable parts, added to undefined concentration effects.

Moreover, if some reference "state" exists (from which one can define "reference RP-values" at each concentration), it will be possible from actual RP-values, to distinguish a viscosity increase associated with increasing of volume concentration, from another viscosity increase resulting from intensified RBC aggregation or from hardening.

(ii) Associated with the overall relaxation time of the system, the shear dependence as function of $\dot{\gamma}^p$ of intrinsic viscosity has allowed to define several classes in highly concentrated disperse systems. Such classes appear closely related to the p-value. As soon as p is determined, one can gain some information about the microstructure of the system (as precise size of particles, for instance), although starting from measurements of macrostructural characteristics.

A fairly good agreement with data has been observed. Nevertheless, further investigations are needed to back up these preliminary results.

Summary

A non-newtonian viscosity equation $\eta_r = (1 - \frac{1}{2} \cdot \tilde{k}\phi)^{-2}$ where ϕ is the volume concentration and $\tilde{k} = (k_0 + k_\infty \dot{\gamma}_r^p)/(1 + \dot{\gamma}_r^p)$ is an intrinsic viscosity, function of a relative shear rate $\dot{\gamma}_r = \dot{\gamma}/\dot{\gamma}_c$, k_0, k_∞ and $\dot{\gamma}_c$ being structural parameters, has been proposed in a previous paper (1). From empirical grounds, the value $p = 1/2$ holds for a large class of systems, like suspensions of rod- and disc-shaped particles. In the high shear rate limit, a *Casson* law-type is recovered and discussed, especially the concentration dependence of the yield stress. However, the latter disappears in the low shear limit, and must be considered as a pseudo-yield stress. Good agreement is found in this low shear limit with some theoretical results of *Bueche* for polymers. More generally, the viscosity equation displays pseudo-plastic behaviour and fitting it on experimental data allows the determination of the structural parameters. Some examples (especially Red Blood Cell suspensions and Blood) are studied and support the model. Nevertheless, for spherical particle suspensions, the best fitting is reached for $p = 1$. Accurate values of particle diameters can be deduced from the structural parameter $\dot{\gamma}_c$, in this case.

Zusammenfassung

In einer vorangegangenen Arbeit (1) wurde eine Viskositätsgleichung für eine nicht-newtonsche Flüssigkeit von der Form $\eta_r = (1 - \frac{1}{2}\tilde{k}\phi)^{-2}$ vorgeschlagen, worin ϕ die Volumenkonzentration und $\tilde{k} = (k_0 + k_\infty \dot{\gamma}_r^p)/(1 + \dot{\gamma}_r^p)$ eine Grenzviskosität bedeutet; die letztere stellt eine Funktion der relativen Schergeschwindigkeit $\dot{\gamma}_r = \dot{\gamma}/\dot{\gamma}_c$ dar, die Konstanten k_0, k_∞ und $\dot{\gamma}_c$ bezeichnen Strukturparameter. Empirisch wird gefunden, daß für eine große Klasse von Systemen, wie z. B. stäbchen- und scheibchenförmigen Teilchen, $p = 1/2$ gilt. In der Grenze hoher Schergeschwindigkeiten wird ein Verlauf gemäß einer Casson-Gleichung gefunden und diskutiert, insbesondere bezüglich der Konzentrationsabhängigkeit der Fließspannung. Allerdings verschwindet diese in der Grenze niedriger Schergeschwindigkeiten und muß daher als Pseudo-Fließspannung betrachtet werden. In diesem Grenzfall wird eine gute Übereinstimmung mit theoretischen Voraussagen von *Bueche* an Polymeren gefunden. Ganz allgemein beschreibt die obige Viskositätsgleichung ein pseudoplastisches Verhalten, und ihre Anpassung an experimentelle Werte erlaubt die Bestimmung der

Strukturparameter. Einige Beispiele, insbesondere Suspensionen von roten Blutkörperchen und Blut, werden untersucht und bestätigen das Modell. Allerdings erhält man bei Suspensionen kugelförmiger Teilchen die beste Anpassung für $p = 1$. In diesem Fall kann man mit Hilfe des Strukturparameters $\dot{\gamma}_c$ genaue Werte der Teilchendurchmesser bestimmen.

References

1) *Quemada, D.*, Rheol. Acta **17**, 632 (1978).

2) *Antonini, G., G. Guiffant, D. Quemada*, J. de Chimie Physique **7**, 1123 (1974).

3) *Antonini, G., G. Guiffant, D. Quemada*, Biorheology, **15**, 111–117 (1978).

4) *Dosne, A. M., C. Merville, L. Drouet. G. Antonini, G. Guiffant, D. Quemada*, Microvascular Research **14**, 45 (1977).

5) *Quemada, D.*, J. de Physique, Coll. C 1, **37**, 9 (1976).

6) *Casson, N.*, in: *C. C. Mills* (ed.), Rheology of Disperse Systems, p. 84, Pergamon Press (London 1959).

7) *Brooks, D. E., J. W. Goodwin, G. V. F. Seaman*, Am. J. Appl. Physiol. **28**, 172 (1970).

8) *Merrill, E. W., W. G. Margetts, G. R. Cokelet, A. Britten, E. W. Salzman, R. E. Pennel, M. Melin*, in: *A. L. Copley* (ed.), Symp. on Biorheol., p. 601, Intersc. Publ. (New York 1964); *Merril, E. W., J. W. Margetts, G. R. Cokelet, E. R. Gilliland*, ibid., p. 135 (1964).

9) *Bueche, F.*, J. Chem. Phys. **22**, 1570 (1974).

10) *Tickner, E. G., A. M. Sacks*, Circulation Res. **25**, 389 (1969).

11) *Chien, S.*, Science **168**, 977 (1970).

12) *Quemada, D.*, Comptes Rendus **282 D**, 1905 (1976).

13) *Chien, S., S. Usami, R. J. Dellenback, C. A. Bryant, M. I. Gregersen*, in: *H. H. Hartet, A. L. Copley* (eds.), Theor. and Clin. Hemorheol., p. 136, Springer-Verlag (Berlin 1971).

14) *Burton, A. C.*, Physiology and Biophysics of the Circulation, Year Book Medic. Publ. (Chicago 1966).

15) *Chien, S., S. A. Luse, K. M. Jan, L. H. Miller, S. Usami, L. H. Miller, H. Fremount*, in: *Ditzel, Lewis* (eds.), Proc. 6th Europ. Conf. on Microcirculation, p. 29–34, Karger (Basel 1971).

16) *Schmid-Schönbein, H.*, Blood Cells **1**, 285 (1975).

17) *Schmid-Schönbein, H., G. Gallasch, E. Volger, H. J. Klose*, Biorheology **10**, 213 (1973).

18) *Schmid-Schönbein, H., R. Wells*, in: *H. H. Hartet, A. Copley* (eds.), Theor. and Clin. Hemorheology, p. 348, Springer-Verlag (Berlin 1971).

19) *Usami, S., S. Chien, M. I. Gregersen*, in: *H. H. Hartet, A. Copley* (eds.), Theor. and Clin. Hemorheology, p. 266 (Berlin 1971).

20) *Schmid-Schönbein, H., R. E. Wells, J. Goldstone*, Biorheology **7**, 227 (1971).

21) *Quemada, D.*, in: *P. Aigrain, P. Nozières* (eds.), De la Thermodynamique à la Géophysique, p. 191–207, CNRS (Paris 1978).

22) *Brooks, D. E., J. W. Goodwin, G. V. F. Seaman*, Biorheology **11**, 69–77 (1974).

23) *Quemada, D.*, in: *C. Klason, J. Kubat* (eds.), Proc. VIIth Intern. Congr. on Rheology, p. 628 (Gothenburg 1976).

24) *Papir, Y. S., I. M. Krieger*, J. Colloid Interface Sci. **34**, 126 (1970).

25) *Quemada, D.*, Rheol. Acta **16**, 82 (1977).

Author's address:

Prof. *D. Quemada*
L.B.H.P.
Université Paris VII
2 Place Jussieux
F-75 221 Paris Cedex 05